nature genetics

De novo mutations in the gene encoding STXBP1 (MUNC18-1) cause early infantile epileptic encephalopathy

Hirotomo Saitsu[1], Mitsuhiro Kato[2], Takeshi Mizuguchi[1], Keisuke Hamada[3], Hitoshi Osaka[4], Jun Tohyama[5], Katsuhisa Uruno[6], Satoko Kumada[7], Kiyomi Nishiyama[1], Akira Nishimura[1], Ippei Okada[1], Yukiko Yoshimura[1], Syu-ichi Hirai[8], Tatsuro Kumada[9], Kiyoshi Hayasaka[2], Atsuo Fukuda[9], Kazuhiro Ogata[3] & Naomichi Matsumoto[1]

Early infantile epileptic encephalopathy with suppression-burst (EIEE), also known as Ohtahara syndrome, is one of the most severe and earliest forms of epilepsy[1]. Using array-based comparative genomic hybridization, we found a *de novo* 2.0-Mb microdeletion at 9q33.3–q34.11 in a girl with EIEE. Mutation analysis of candidate genes mapped to the deletion revealed that four unrelated individuals with EIEE had heterozygous missense mutations in the gene encoding syntaxin binding protein 1 (*STXBP1*). STXBP1 (also known as MUNC18-1) is an evolutionally conserved neuronal Sec1/Munc-18 (SM) protein that is essential in synaptic vesicle release in several species[2–4]. Circular dichroism melting experiments revealed that a mutant form of the protein was significantly thermolabile compared to wild type. Furthermore, binding of the mutant protein to syntaxin was impaired. These findings suggest that haploinsufficiency of *STXBP1* causes EIEE.

EIEE, also known as Ohtahara syndrome[1], is characterized by early onset of tonic spasms, seizure intractability, a characteristic suppression-burst pattern on the electroencephalogram (EEG) and poor outcome with severe psychomotor retardation[5,6]. Many causes have been considered for EIEE. Structural abnormalities of the brain such as hemimegalencephaly, Aicardi syndrome and porencephaly often cause EIEE, but cryptogenic or idiopathic EIEE is found in a subset of individuals, in whom genetic factors could be involved[5,6]. The transition from EIEE to West syndrome, which is characterized by tonic spasms with clustering, arrest of psychomotor development and hypsarrhythmia on the EEG, occurs in 75% of individuals with EIEE[5,6]. A common pathological mechanism linking these two syndromes has been suggested. Consistent with this idea, specific mutations of the *ARX* (aristaless-related homeobox) gene at Xp22.13 have been recently found in male subjects with EIEE and West syndrome[7,8]. In most cryptogenic EIEE cases, however, the genetic cause remains to be elucidated.

Microarray technologies detect genomic copy number alterations, which may be related to disease phenotypes, at a submicroscopic level[9,10]. In a BAC array-based comparative genomic hybridization (aCGH) analysis (containing 4,219 clones with 0.7-Mb resolution for genome-wide analysis) of individuals with mental retardation, we found a microdeletion at 9q33.3–q34.11 in a girl with EIEE (subject 1) (**Fig. 1a**). The deletion was 2.0 Mb in size and was confirmed by fluorescent *in situ* hybridization (FISH) analysis on the subject's chromosomes (**Fig. 1b**), whereas no deletion was found in her parents (data not shown).

More than forty genes mapped within the deletion (**Fig. 1b**). Among them, the gene encoding syntaxin binding protein 1 (STXBP1, also known as MUNC18-1) was of interest because mouse *Stxbp1* has been shown to be essential for synaptic vesicle release[2], and it is specifically expressed in the brains of rodents and humans[11,12]. We screened for *STXBP1* mutations in 13 unrelated individuals with EIEE. A total of four heterozygous missense mutations were found in three males and a female (**Table 1**): 251T>A (V84D) (subject 11), 539G>A (C180Y) (subject 6), 1328T>G (M443R) (subject 7) and 1631G>A (G544D) (subject 3) (**Fig. 2**). All mutations occurred at evolutionary conserved amino acids (**Fig. 2**). Parental DNAs were available except for subject 3, whose father was deceased. *STXBP1* mutations in subjects 6, 7 and 11 were *de novo* events, as their parents did not possess the same nucleotide

[1]Department of Human Genetics, Yokohama City University Graduate School of Medicine, 3-9 Fukuura, Kanazawa-ku, Yokohama 236-0004, Japan. [2]Department of Pediatrics, Yamagata University School of Medicine, 2-2-2 Iida-nishi, Yamagata 990-9585, Japan. [3]Department of Biochemistry, Yokohama City University Graduate School of Medicine, 3-9 Fukuura, Kanazawa-ku, Yokohama 236-0004, Japan. [4]Division of Neurology, Clinical Research Institute, Kanagawa Children's Medical Center, 2-138-4 Mutsukawa, Minami-ku, Yokohama 232-8555, Japan. [5]Department of Pediatrics, Epilepsy Center, Nishi-Niigata Chuo National Hospital, 1-14-1 Masago, Nishi-ku, Niigata 950-2085, Japan. [6]Epilepsy Center, Yamagata National Hospital, 126-2 Gyosai, Yamagata 990-0876, Japan. [7]Department of Neuropediatrics, Tokyo Metropolitan Neurological Hospital, 2-6-1 Musashidai, Fuchu 183-0042, Japan. [8]Department of Molecular Biology, Yokohama City University Graduate School of Medicine, 3-9 Fukuura, Kanazawa-ku, Yokohama 236-0004, Japan. [9]Department of Physiology, Hamamatsu University School of Medicine, 1-20-1 Handayama, Hamamatsu 431-3192, Japan. Correspondence should be addressed to H.S. (hsaitsu@yokohama-cu.ac.jp) or N.M. (naomat@yokohama-cu.ac.jp).

Received 8 February; accepted 17 March; published online 11 May 2008; doi:10.1038/ng.150

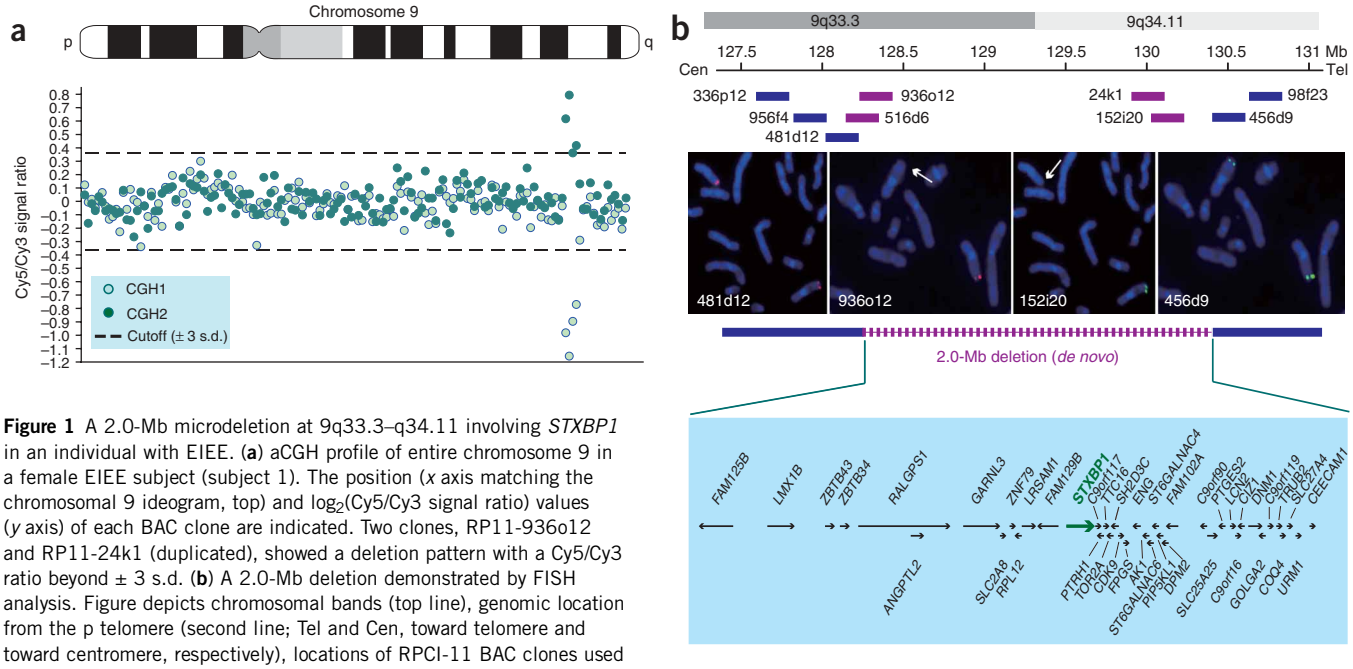

Figure 1 A 2.0-Mb microdeletion at 9q33.3–q34.11 involving *STXBP1* in an individual with EIEE. (**a**) aCGH profile of entire chromosome 9 in a female EIEE subject (subject 1). The position (*x* axis matching the chromosomal 9 ideogram, top) and $\log_2$(Cy5/Cy3 signal ratio) values (*y* axis) of each BAC clone are indicated. Two clones, RP11-936o12 and RP11-24k1 (duplicated), showed a deletion pattern with a Cy5/Cy3 ratio beyond ± 3 s.d. (**b**) A 2.0-Mb deletion demonstrated by FISH analysis. Figure depicts chromosomal bands (top line), genomic location from the p telomere (second line; Tel and Cen, toward telomere and toward centromere, respectively), locations of RPCI-11 BAC clones used for FISH (purple, deleted; dark blue, not deleted), and FISH images of four clones (RP11-481d12, RP11-936o12, RP11-152i20 and RP11-456d9) hybridized to the subject's chromosomes. White arrows, deletion. A total of 41 RefSeq genes, including *STXBP1*, are mapped within the 2.0-Mb region (bottom).

changes. Parentage was confirmed using several microsatellite markers (data not shown). All of the nucleotide changes were absent in 250 healthy Japanese controls (500 chromosomes).

Clinical features of the subjects with EIEE having *STXBP1* defects are summarized in **Table 1** (see also **Supplementary Note** online). Subject 1 has been previously described[13]. Brain magnetic resonance imaging (MRI) did not detect any apparent structural anomalies or hippocampal abnormalities, but showed some atrophy (**Fig. 3a–e**). Three subjects (subjects 1, 6 and 7) showed delayed myelination or hypomyelination[13] (**Fig. 3b–d**). Suppression-burst patterns on EEGs were recognized in all subjects (**Fig. 3f**). Tonic spasms developed 10 d to 3 months after birth (**Supplementary Video 1** online for subject 7). In four subjects (subjects 1, 6, 7 and 11), transition from EIEE to West syndrome with hypsarrhythmia on the EEG occurred (**Fig. 3g**). In subject 3, the EEG at 35 years of age showed independent or synchronized focal spikes, or sharp waves in the bilateral frontal area (**Fig. 3h**). We did not observe any differences of clinical symptoms between mutation-positive and mutation-negative subjects.

All four mutant proteins have amino acid replacements in the hydrophobic core of STXBP1 that would be considered to destabilize their folding architecture; in particular, three of the mutants (V84D, G544D and M443R) have replaced the wild-type (WT) residues with charged residues that would be predicted to severely disrupt the conformation of STXBP1 (**Fig. 4a**)[14]. Thus, the mutated proteins are likely to be structurally unstable. To examine properties of the mutant STXBP1 proteins, we purified recombinant WT and mutant proteins using the GST-tag method. Circular dichroism spectra revealed that the helical content of the C180Y mutant was slightly lower (39%) than that of WT (43%), suggesting that the mutation destabilized the secondary structure of STXBP1 (**Fig. 4b**)[15]. Moreover, circular-dichroism melting experiments showed that the C180Y mutation lowered the thermostability of STXBP1. The obtained melting (transition midpoint) temperature (T_m) of the C180Y mutant was about 11 °C lower than that of the WT (49.53 ± 0.03 °C for the WT and the 38.54 ± 0.03 °C for the C180Y mutant) (**Fig. 4c**). As the T_m of the C180Y mutant is close to the physiological temperature of human body, its functional activity is less likely to be retained in human brain. Although gel filtration experiments showed that the purified C180Y mutant existed as a monomer as did the wild-type (data not shown), other STXBP1 mutants (V84D, G544D and M443R) easily tended to form aggregates, and thus we did not obtain sufficient amounts of these proteins for biophysical analyses. Furthermore, transient expression in Neuroblastoma 2A cells revealed that all of the mutant STXBP1 proteins (V84D, C180Y, M443R and G544D), but not WT-STXBP1, tended to aggregate (**Supplementary Fig. 1** online), suggesting that all of the mutant proteins are structurally unstable.

It has been reported that Stxbp1 regulates synaptic vesicle release, at least in part, by binding to syntaxin 1A (Stx1a) as well as to the SNARE complex directly[16,17]. Stxbp1 binds to Stx1a in two different ways: binding to a closed form of Stx1a and binding to the N terminus of an open form of Stx1a compatible with SNARE complex formation[16–18]. The interaction with the N terminus of open-form Stx1a is important in synaptic vesicle release, whereas interaction with closed-form Stx1a is involved in synaptic vesicle docking[16–19]. Thus, we examined whether the C180Y mutant could bind to the closed and/or open forms of STX1A, using the GST pull-down assay at 4 °C. WT STXBP1 bound to both closed and open forms of GST-STX1A at comparable levels; the C180Y mutant showed decreased binding to both forms of GST-STX1A, particularly the open one, compared to WT STXBP1 (**Fig. 4d,e**). Thus, we would expect synaptic vesicle release to be greatly impaired in the individual with the C180Y substitution.

We identified one complete deletion and four missense mutations of *STXBP1* in individuals with EIEE (three male and two female). STXBP1 is a member of the evolutionary conserved SM gene family that acts at specific steps of intracellular membrane transport[20,21]. In

Table 1 Summary of clinical features of EIEE subjects with *STXBP1* defects

Subject	Sex	*STXBP1* defect	Initial symptoms	Age at onset of spasms	Initial EEG	Age at transition to West syndrome	Response to therapy; frequency of medication	Development	Neurological examination	MRI	Ref.
1	F	Deletion	Tonic seizure and oral automatism	2 mo	Suppression-burst	3 mo	Seizure free from 5 mo after TRH injection	Poor visual attention No rolling over	Profound MR Hypotonic quadriplegia	Cortical atrophy Diffuse hypomyelination Thin corpus callosum (at 12 mo)	Ref. 13
3	M	1631G>A (G544D)	Blinking	10 d	Suppression-burst	–	Seizure free from 3 mo	Walking at 7 yr A few words Feeds self	Profound MR Mild spastic diplegia	Normal (at 37 yr)	–
6	M	539G>A (C180Y)	Tonic seizure with blinking	3 mo	Suppression-burst	4 mo	Intractable; daily	Weak eye pursuit No smile No head control	Profound MR Severe spastic quadriplegia	Mild atrophic change Delayed myelination (at 3 mo)	–
7	F	1328T>G (M443R)	Upward gazing and tonic seizure	2 mo	Suppression-burst	4 mo	Intractable; hourly TRH injection temporarily effective	No head control No words	Profound MR Mild spastic quadriplegia	Mild atrophic change Delayed myelination (at 13 mo)	–
11	M	251T>A (V84D)	Spasms and tonic-clonic seizure	2 mo	Suppression-burst	9 mo	Intractable, daily	No head control No words	Profound MR Severe hypotonic quadriplegia Choreoathetosis	Mild atrophic change of frontal lobe (at 8 yr)	–

MR, mental retardation; TRH, thyrotropin-releasing hormone; mo, month(s); yr, year(s).

Figure 2 Heterozygous mutations of *STXBP1* found in individuals with EIEE. Schematic representation of *STXBP1* consisting of 20 exons (rectangles). There are two isoforms: isoform a (GenBank accession number, NM_003165) with exon 19, and isoform b (NM_001032221) without exon 19 of isoform a. UTR, coding region, and SEC1 domain are dark blue, white and sky blue, respectively. All of the missense mutations occurred at evolutionary conserved amino acids in the SEC1 domain. Three mutations were confirmed as *de novo*; the other could not be confirmed, as the father was deceased. Homologous sequences were aligned using the CLUSTALW web site.

mammalian exocytosis, the vesicular SNARE protein, VAMP2 (synaptobrevin2), and the target membrane SNARE proteins, Syntaxin-1 and SNAP25, constitute the core fusion machinery that brings two membranes into close apposition to fuse[17,22]. Stxbp1 was first identified as a protein interacting with Syntaxin-1A (ref. 23), and its null mutation leads to complete loss of neurotransmitter secretion from synaptic vesicles throughout development in mice, though seizures have never been described[2]. Thus, STXBP1 is very likely to play a central role for synaptic vesicle release in coordination with SNARE proteins. Knowledge of the genetic bases of epilepsies is increasing rapidly, but most genes associated with epilepsy syndromes are ion channel genes[24]. A mutation in the gene encoding synapsin I, a synaptic vesicle protein thought to regulate the kinetics of neurotransmitter release during priming of synaptic vesicles, has been identified in a family with X-linked epilepsy and learning difficulties[25]. This is the second report implicating aberrations in genes involved in synaptic vesicle release in epilepsy.

All four of the mutant STXBP1 proteins seemed to be structurally unstable because of their amino acid replacements in the hydrophobic core[14]. In fact, in the case of the C180Y mutant STXBP1, its thermal instability occurred near body temperature, and its impaired binding to the open form of STX1A implies that the mutation is hypomorphic or amorphic with regard to synaptic vesicle release. It is also known that *Stxbp1* heterozygous knockout mice show impaired synaptic function owing to reduced size and replenishment rate of readily releasable vesicles[26], suggesting that the functionally impaired STXBP1 may affect synaptic function in the human brain. Considering that the microdeletion involving *STXBP1* also resulted in EIEE, haploinsufficiency of *STXBP1* is the likely cause of EIEE.

It is unknown how haploinsufficiency of *STXBP1* leads to EIEE. EIEE is commonly associated with various structural brain

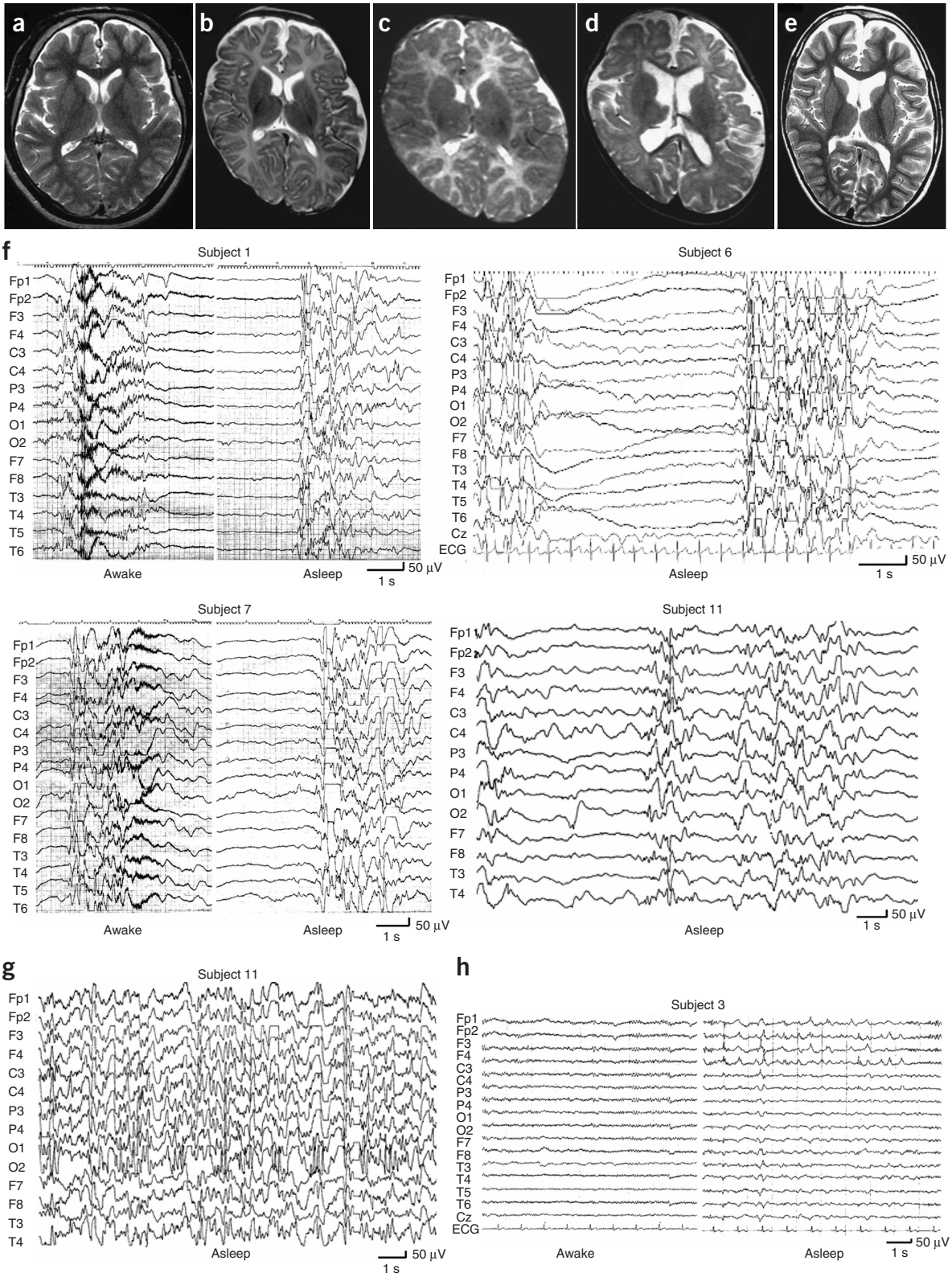

Figure 3 Brain MRI and EEG of subjects with EIEE having *STXBP1* defects. (**a**–**e**) Brain MRI T2-weighted axial images through the basal ganglia showing normal brain structure in the subjects with *STXBP1* mutation (**a**, subject 3 at age of 37 years of age; **b**, subject 6 at 3 months; **c**, subject 7 at 3 months; **d**, subject 7 at 13 months; **e**, subject 11 at 8 years). (**f**) Suppression-burst on interictal EEG of subjects 1 (at age 2 months), 6 (at 3 months), 7 (at 2 months) and 11 (at 3 months). High-voltage bursts alternate with almost flat suppression phases at an approximately regular rate in both awake and asleep states. (**g**) Hypsarrhythmia on interictal EEG of the subject 11 at age of 8 years. Transition from EIEE to West syndrome was recognized at age of 9 months. (**h**) EEG of the 35-year-old subject 3, showing focal spikes or sharp waves in the bilateral frontal area during sleep.

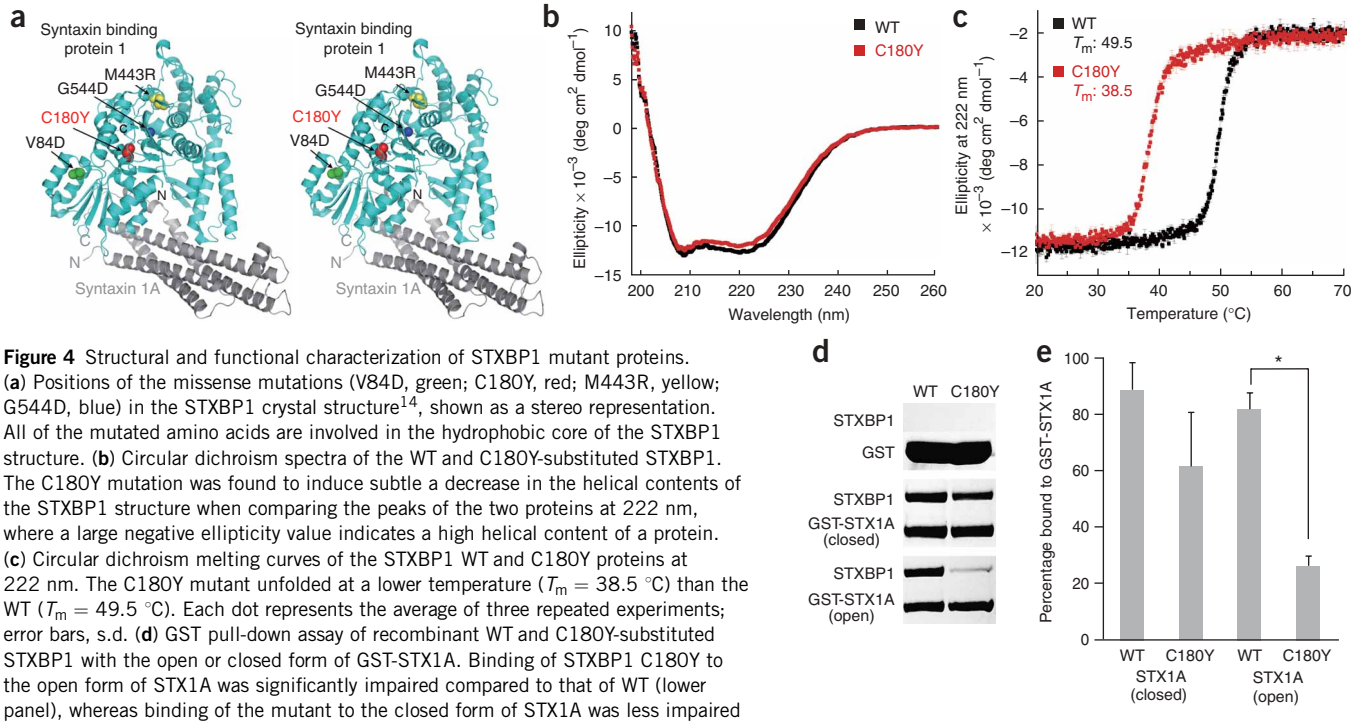

Figure 4 Structural and functional characterization of STXBP1 mutant proteins. (**a**) Positions of the missense mutations (V84D, green; C180Y, red; M443R, yellow; G544D, blue) in the STXBP1 crystal structure[14], shown as a stereo representation. All of the mutated amino acids are involved in the hydrophobic core of the STXBP1 structure. (**b**) Circular dichroism spectra of the WT and C180Y-substituted STXBP1. The C180Y mutation was found to induce subtle a decrease in the helical contents of the STXBP1 structure when comparing the peaks of the two proteins at 222 nm, where a large negative ellipticity value indicates a high helical content of a protein. (**c**) Circular dichroism melting curves of the STXBP1 WT and C180Y proteins at 222 nm. The C180Y mutant unfolded at a lower temperature (T_m = 38.5 °C) than the WT (T_m = 49.5 °C). Each dot represents the average of three repeated experiments; error bars, s.d. (**d**) GST pull-down assay of recombinant WT and C180Y-substituted STXBP1 with the open or closed form of GST-STX1A. Binding of STXBP1 C180Y to the open form of STX1A was significantly impaired compared to that of WT (lower panel), whereas binding of the mutant to the closed form of STX1A was less impaired (middle panel). In a control experiment, neither WT nor C180Y STXBP1 showed any binding to GST alone (upper panel). (**e**) Quantitative analysis of the interaction between STXBP1 and GST-STX1A based on the data shown in **d**. *P = 0.000148 by unpaired Student's t-test, two-tailed. Averages of three repeated experiments; error bars, s.d.

abnormalities[5,6], but we did not recognize any in the five subjects with EIEE having *STXBP1* defects. Suppression-burst pattern on the EEG has been observed in individuals with cerebral conditions disconnecting the cortex from deep structures, such as deep brain tumors, stroke with severe anoxia and barbiturate anesthesia[1,27]. Tonic seizures in EIEE have been suggested to originate from subcortical structures, especially the brainstem[5]. Notably, although normal brain architecture develops in *Stxbp1* null mice, extensive cell death of mature neurons occurs first in lower brain areas, and the lower brainstem is almost completely lost by embryonic day 18 (ref. 2). Thus, in addition to the impaired synaptic vesicle release, neuronal cell death in the brainstem might contribute to EIEE pathogenesis, although brain MRI did not show brainstem abnormalities in individuals with aberrant *STXBP1*. Delayed myelination or hypomyelination in subjects 1, 6 and 7 may also affect corticosubcortical connections.

In conclusion, we have identified heterozygous mutations of *STXBP1* at 9q34.11 in individuals with EIEE. It is noteworthy that autosomal *STXBP1* abnormalities can explain EIEE in both sexes. Understanding the abnormal synaptic vesicle release underlying EIEE may provide new insights for intractable spasms in infancy.

METHODS

Subjects. We analyzed a total of 14 Japanese individuals with EIEE. The diagnosis was made on the basis of clinical features, including early onset of tonic spasms, seizure intractability and psychomotor retardation as well as characteristic suppression-burst pattern on the EEG. Experimental protocols were approved by the Committee for Ethical Issues at Yokohama City University School of Medicine. Informed consent was obtained for all individuals included in this study in agreement with the requirements of Japanese regulations. Clinical histories of subjects with *STXBP1* aberrations are described in **Table 1** and **Supplementary Note**, except for subject 1, whose clinical information has been previously reported (as no. 2)[13].

Microarray analysis. We developed a BAC array containing 4,219 BAC clones spanning the entire human genome. We selected 5,042 BAC/PAC (phage P1-derived artificial chromosome) clones using the University of California Santa Cruz (UCSC) Genome Browser (2003 July version), with spacing at every 0.7 Mb of the human genome, and chose for arrays 4,219 clones that showed a unique FISH signal at the predicted chromosomal location. The other 822 clones were not spotted on slides, as 438 (8.7%) yielded more than one chromosomal signal by FISH and 384 (7.6%) showed a signal on a different chromosome that was probably due to contamination in our laboratory. The 4,219 clones also included 59 BAC/PAC clones previously used for a microarray targeting all chromosomal subtelomeres and critical regions for mental retardation syndromes[28]. BAC/PAC DNA was extracted using an automatic DNA extraction system PI-100 (Kurabo), amplified by two-round PCR, purified and adjusted to the final concentration >500 ng/μl, and spotted in duplicate on CodeLink activated slides (Amersham) by the ink-jet spotting method (Nihon Gaishi).

aCGH analysis was performed as described previously[29]. Briefly, after complete digestion using DpnII, subject's DNA was labeled in experiment 1 (CGH1) with Cy-5 dCTP (GE Healthcare) and control DNA was labeled with Cy-3 dCTP (GE Healthcare) using the BioPrime Array CGH Genomic Labeling System (Invitrogen). To rule out false positives, dyes were swapped in CGH2 (subject's DNA with Cy3 and control DNA with Cy5) to check whether the signal patterns obtained in CGH1 were reversed. After drying, the arrays were scanned by GenePix 4000B (Axon Instruments) and analyzed using GenePix Pro 6.0 (Axon Instruments). The signal intensity ratio between the subject's and the control DNA was calculated from the data of the single-slide experiment in each of CGH1 and CGH2, using the ratio of means formula (F635 mean – B635 median / F532 mean – B532 median, where 'F635 mean' is the mean of all the feature pixel intensities at 635 nm, 'B635 median' is the median of all the background pixel intensities at 635 nm, and 'F532 mean' and 'B532 median' are defined similarly at 532 nm) according to GenePix Pro. 6.0. The s.d. of each clone was then calculated. The signal ratio was regarded as 'abnormal' if it ranged outside ± 3 s.d. in both CGH1 and CGH2, with opposite directions.

FISH analysis. BAC/PAC DNA was labeled with SpectrumGreen-11-dUTP or SpectrumOrange-11-dUTP (Vysis) by nick translation and denatured at 70 °C for 10 min. Probe-hybridization mixtures (15 µl) were applied to chromosomes, incubated at 37 °C for 16–72 h, then washed and mounted in antifade solution (Vector) containing 4,6-diamidino-2-phenylindole (DAPI). Photographs were taken on an AxioCam MR CCD fitted to Axioplan2 fluorescence microscope (Carl Zeiss).

Mutation screening. Genomic DNA was obtained from peripheral blood leukocytes according to standard protocols. DNA for mutation screening was amplified using Genomiphi version 2 (GE Healthcare). Mutation screening of exons 1 to 20 covering the *STXBP1* coding region was performed by high resolution melt analysis. Real-time PCR and subsequent high-resolution melt analysis were performed in 12-µl mixture on RoterGene-6200 HRM (Corbett Life Science). For exons 2 to 20, the PCR mixture contained 1× ExTaq buffer, 0.2 mM each dNTP, 0.2 µM each primer, 1 µl DMSO, 1 µl LCGreen Plus (Idaho Technology) and 0.25 U ExTaqHS polymerase (Takara). For exon 1, the PCR mixture contained 1× GC buffer II, 0.4 mM each dNTP, 0.2 µM each primer, 1 µl LCGreen Plus (Idaho Technology) and 0.5 U LA Taq polymerase (Takara). PCR conditions and primer sequences are showed in **Supplementary Table 1** online. If a sample showed an aberrant melting curve pattern, the PCR product was purified with ExoSAP (USB) and sequenced for both forward and reverse strands with BigDye Terminator chemistry version 3 according to the standard protocol (Applied Biosystems). The reaction mixture was purified using Sephadex G-50 (GE Healthcare) and Multiscreen-96 (Millipore). Sequences were obtained on the ABI Genetic Analyzer 3100 (Applied Biosystems) with sequence analysis software version 5.1.1 (Applied Biosystems) and SeqScape version 2.1.1 (Applied Biosystems). All mutations were also verified on PCR products directly using genomic DNA as a template.

Parentage testing. For all families showing *de novo* mutations, we confirmed parentage by microsatellite analysis using ABI Prism linkage mapping set version 2.5, MD10 (Applied Biosystems). We chose 12 probes for screening (*D6S422*, *D7S493*, *D8S285*, *D9S161*, *D10S208*, *D11S987*, *D12S345*, *D16S503*, *D17S921*, *D18S53*, *D19S220* and *D20S196*), and considered biological parents confirmed if more than four informative markers were compatible in each family.

Expression vectors. A full-length human *STXBP1* cDNA clone (amino acids 1–594, GenBank accession number BC015749) and *STX1A* cDNA clone (amino acids 1–288, accession number BC064644) were purchased from Invitrogen. *STXBP1* and *STX1A* (amino acids 1–263, cytoplasmic domain as a closed form) cDNAs were cloned into pGEX6P-3 (GE Healthcare) to generate glutathione S-transferase (GST) fusion proteins. Site-directed mutagenesis was performed using a KOD-Plus-Mutagenesis kit (Toyobo) according to the manufacturer's protocol to generate *STXBP1* mutants including 251T>A (V84D), 539G>A (C180Y), 1328T>G (M443R) and 1631G>A (G544D). To produce an open form of STX1A, we generated L165A E166A double mutants[30] by site-directed mutagenesis using a KOD-Plus-Mutagenesis kit (Toyobo). All variant cDNAs were verified by sequencing.

Protein expression, purification and binding assay. Protein expression was performed in *Escherichia coli* BL21 (DE3). Bacteria were grown at 37 °C in Terrific Broth media with 300 µg/ml ampicillin to a density yielding an absorbance at 600 nm of 0.8, then protein expression was induced with 0.5 mM isopropyl-β-D-thiogalactoside (IPTG) at 20 °C (WT STXBP1, STX1A) or 18 °C (C180Y mutant of STXBP1) overnight. Cells were collected by centrifugation and lysed using a French press (SLM Aminco). Proteins were purified by affinity chromatography using Glutathione Sepharose High Performance (GE Healthcare). GST tags of STXBP1 were removed by digestion with human rhinovirus 3C protease at 4 °C. STXBP1 was further purified by HiTrap Q HP (GE Healthcare) and Superdex-75 (GE Healthcare) columns in a buffer containing 200 mM NaCl, 20 mM sodium phosphate buffer, pH 7.5 and 1 mM dithiothreitol (DTT).

For the GST pull-down assay to measure the binding activity of STXBP1 (WT or C180Y mutant), we prepared glutathione Sepharose 4B column beads (GE Healthcare) bound to either GST or GST-STX1A protein (closed or open form). Seven micrograms of STXBP1 (WT or C180Y mutant) proteins were incubated for 1 h at 4 °C with gentle agitation in a binding buffer containing 200 mM NaCl, 20 mM sodium phosphate buffer, pH 7.5, 1 mM DTT and 0.1% Triton X-100. The beads were collected by centrifugation and washed rapidly four times with binding buffer. The bound molecules were eluted with a buffer containing 300 mM NaCl, 20 mM sodium phosphate buffer, pH 7.5, 5 mM DTT, 1 mM EDTA and 16 mM reduced glutathione. The eluted fractions were analyzed by SDS-PAGE, and protein bands were visualized by staining with Coomassie brilliant blue. The protein bands were analyzed by quantitative densitometry using a FluorChem 8900 (Alpha Inntech). Experiments were repeated three times. The STX1A-binding activities of STXBP1 (WT or C180Y mutant) were estimated as density ratios of STXBP1 and GST-STX1A in the eluted samples. Statistical analyses were done using the unpaired Student's *t*-test (two-tailed).

Circular dichroism measurements. We measured far-UV circular dichroism spectra using a J725 spectropolarimeter (Jasco) equipped with a thermoelectric temperature control system (Peltier). All data were collected using a quartz cuvette with a path length of 1 mm and a spectral bandwidth of 1 nm. The experiments were performed in 20 mM sodium phosphate buffer, pH 7.5, containing 200 mM NaCl and 1 mM DTT. The protein concentration was 5 µM for wavelength scans and 2.5 µM for temperature scans. For wavelength scan experiments, the ellipticity was scanned from 300 to 198 nm at 4 °C. Averages of three scans were recorded. Spectra were corrected for contributions of buffer solution. The secondary structure was estimated using the Yang method[15] encoded in the software bundled with the circular dichroism instrument. For temperature scan experiments, a change of ellipticity at a wavelength of 222 nm was monitored at a scan rate of 0.75 K/min from 20 to 70 °C. T_m was calculated by fitting a sigmoid-function equation using KaleidaGraph (Synergy Software). The data from three independent experiments were averaged and the s.d. calculated.

URLs. UCSC Genome Browser, http://genome.ucsc.edu/cgi-bin/hgGateway; CLUSTALW, http://align.genome.jp/.

Accession codes. GenBank: human syntaxin binding protein 1 mRNA (*STXBP1*) isoform a, NM_003165; *STXBP1* mRNA isoform b, NM_001032221. Protein Data Bank: neuronal-Sec1-syntaxin 1a complex crystal structure, 1DN1. Gene Expression Omnibus: aCGH data have been deposited with accession code GSE10077.

Note: Supplementary information is available on the Nature Genetics website.

ACKNOWLEDGMENTS

We thank subjects and their families for their participation in this study. This work was supported by Research Grants from the Ministry of Health, Labour and Welfare (N.M.) and a Grant-in-Aid for Scientific Research on Priority Areas from the Ministry of Education, Culture, Sports, Science and Technology of Japan (N.M.).

AUTHORS CONTRIBUTIONS

H.S. and N.M. designed and directed the study and wrote the manuscript; M.K., H.O., J.T., K.U., S.K. and K. Hayasaka collected samples and provided clinical information of the subjects; T.M. performed aCGH and FISH analysis; H.S., K.N., A.N., I.O. and Y.Y. provided gene sequences of the subjects; H.S., S.-i.H., T.K. and A.F. did transfection experiments; and H.S., K. Hamada and K.O. performed protein functional and structural analyses.

Published online at http://www.nature.com/naturegenetics
Reprints and permissions information is available online at http://npg.nature.com/reprintsandpermissions

1. Ohtahara, S. *et al.* On the specific age dependent epileptic syndrome: the early-infantile epileptic encephalopathy with suppression-burst [in Japanese with English abstract]. *No To Hattatsu* **8**, 270–279 (1976).
2. Verhage, M. *et al.* Synaptic assembly of the brain in the absence of neurotransmitter secretion. *Science* **287**, 864–869 (2000).
3. Harrison, S.D., Broadie, K., van de Goor, J. & Rubin, G.M. Mutations in the Drosophila *Rop* gene suggest a function in general secretion and synaptic transmission. *Neuron* **13**, 555–566 (1994).
4. Weimer, R.M. *et al.* Defects in synaptic vesicle docking in unc-18 mutants. *Nat. Neurosci.* **6**, 1023–1030 (2003).

5. Djukic, A., Lado, F.A., Shinnar, S. & Moshe, S.L. Are early myoclonic encephalopathy (EME) and the Ohtahara syndrome (EIEE) independent of each other? *Epilepsy Res.* **70** (suppl. 1), S68–S76 (2006).
6. Ohtahara, S. & Yamatogi, Y. Ohtahara syndrome: with special reference to its developmental aspects for differentiating from early myoclonic encephalopathy. *Epilepsy Res.* **70**, S58–S67 (2006).
7. Kato, M., Das, S., Petras, K., Sawaishi, Y. & Dobyns, W.B. Polyalanine expansion of ARX associated with cryptogenic West syndrome. *Neurology* **61**, 267–276 (2003).
8. Kato, M. *et al.* A longer polyalanine expansion mutation in the *ARX* gene causes early infantile epileptic encephalopathy with suppression-burst pattern (Ohtahara syndrome). *Am. J. Hum. Genet.* **81**, 361–366 (2007).
9. Vissers, L.E.L.M., Veltman, J.A., van Kessel, A.G. & Brunner, H.G. Identification of disease genes by whole genome CGH arrays. *Hum. Mol. Genet.* **14**, R215–R223 (2005).
10. Feuk, L., Marshall, C.R., Wintle, R.F. & Scherer, S.W. Structural variants: changing the landscape of chromosomes and design of disease studies. *Hum. Mol. Genet.* **15**, R57–R66 (2006).
11. Garcia, E.P., Gatti, E., Butler, M., Burton, J. & De Camilli, P. A rat brain Sec1 homologue related to Rop and UNC18 interacts with syntaxin. *Proc. Natl. Acad. Sci. USA* **91**, 2003–2007 (1994).
12. Kalidas, S. *et al.* Expression of p67 (Munc-18) in adult human brain and neuroectodermal tumors of human central nervous system. *Acta Neuropathol.* **99**, 191–198 (2000).
13. Tohyama, J. *et al.* Early onset West syndrome with cerebral hypomyelination and reduced cerebral white matter. *Brain Dev.* **30**, 349–355 (2008).
14. Misura, K.M.S., Scheller, R.H. & Weis, W.I. Three-dimensional structure of the neuronal-Sec1-syntaxin 1a complex. *Nature* **404**, 355–362 (2000).
15. Yang, J.T., Wu, C.S. & Martinez, H.M. Calculation of protein conformation from circular dichroism. *Methods Enzymol.* **130**, 208–269 (1986).
16. Dulubova, I. *et al.* Munc18–1 binds directly to the neuronal SNARE complex. *Proc. Natl. Acad. Sci. USA* **104**, 2697–2702 (2007).
17. Toonen, R.F. & Verhage, M. Munc18–1 in secretion: lonely Munc joins SNARE team and takes control. *Trends Neurosci.* **30**, 564–572 (2007).
18. Rickman, C., Medine, C.N., Bergmann, A. & Duncan, R.R. Functionally and spatially distinct modes of munc18-syntaxin 1 interaction. *J. Biol. Chem.* **282**, 12097–12103 (2007).
19. Shen, J., Tareste, D.C., Paumet, F., Rothman, J.E. & Melia, T.J. Selective activation of cognate SNAREpins by Sec1/Munc18 proteins. *Cell* **128**, 183–195 (2007).
20. Weimer, R.M. & Richmond, J.E. Synaptic vesicle docking: a putative role for the Munc18/Sec1 protein family. *Curr. Top. Dev. Biol.* **65**, 83–113 (2005).
21. Sudhof, T.C. The synaptic vesicle cycle. *Annu. Rev. Neurosci.* **27**, 509–547 (2004).
22. Rizo, J. & Sudhof, T.C. Snares and Munc18 in synaptic vesicle fusion. *Nat. Rev. Neurosci.* **3**, 641–653 (2002).
23. Hata, Y., Slaughter, C.A. & Sudhof, T.C. Synaptic vesicle fusion complex contains unc-18 homologue bound to syntaxin. *Nature* **366**, 347–351 (1993).
24. Gurnett, C.A. & Hedera, P. New ideas in epilepsy genetics: novel epilepsy genes, copy number alterations, and gene regulation. *Arch. Neurol.* **64**, 324–328 (2007).
25. Garcia, C.C. *et al.* Identification of a mutation in synapsin I, a synaptic vesicle protein, in a family with epilepsy. *J. Med. Genet.* **41**, 183–186 (2004).
26. Toonen, R.F. *et al.* Munc18–1 expression levels control synapse recovery by regulating readily releasable pool size. *Proc. Natl. Acad. Sci. USA* **103**, 18332–18337 (2006).
27. Spreafico, R. *et al.* Burst suppression and impairment of neocortical ontogenesis: electroclinical and neuropathologic findings in two infants with early myoclonic encephalopathy. *Epilepsia* **34**, 800–808 (1993).
28. Harada, N. *et al.* Subtelomere specific microarray based comparative genomic hybridisation: a rapid detection system for cryptic rearrangements in idiopathic mental retardation. *J. Med. Genet.* **41**, 130–136 (2004).
29. Miyake, N. *et al.* BAC array CGH reveals genomic aberrations in idiopathic mental retardation. *Am. J. Med. Genet. A.* **140**, 205–211 (2006).
30. Dulubova, I. *et al.* A conformational switch in syntaxin during exocytosis: role of munc18. *EMBO J.* **18**, 4372–4382 (1999).